

GPO PRICE \$ \_\_\_\_\_

CESTI PRICE(S) \$ \_\_\_\_\_

1200

CC

1965 11 15



**CENTER FOR SPACE RESEARCH**  
**MASSACHUSETTS INSTITUTE OF TECHNOLOGY**



AGILITY FORM 802

N66 30751	(THRU)
(ACCESSION NUMBER)	(CODE)
34	07
(PAGES)	(CATEGORY)
CR-76257	
(NASA CR OR TMX CR AD NUMBER)	

ORGANIZATION OF A DIPOLE  
PHASED ARRAY ANTENNA

by

L. A. Jacobson

CSR TR-66-4

*NAS-249*

## GLOSSARY

d	Spacing between dipole elements.
$\rho_{el}$	Elevation angle of incoming or outgoing wave front.
$\rho_{az}$	Azimuth angle of incoming or outgoing wave front.
$\phi_x$ or $\rho_x$	Relative phase along x axis.
$\phi_y$ or $\rho_y$	Relative phase along y axis.
M	Multiplicity or number of branches stemming from each node.
$N_D$	Number of dipoles in square array.
L	Number of distribution levels when $M^L = N_D$ .
$D_{N_1, N_2 \dots N_L}$	Location of particular dipole.
N	Number of $\frac{\pi}{2}$ radius in node departure angle.
k	Order of level $1 < k < L$ .
q	Number of bits controlling phase shifts; also LSB prior to truncation.
P	Index integer 0, 1, 2, . . .
$N_p$	Number of phase shifts in array.
$G_M$	Total wire length in single cell of multiplicity M.
$W_M$	Total wire length in array of multiplicity M.
A	Expensive operational block of computer.
B	Less expensive operational block of computer.

## INTRODUCTION

A unique dipole phased array antenna has been proposed\* which utilizes micro electronics distributed throughout the array. The objective of this paper is to discuss the initial signal processing and logical organization of the distributed system. Some of the relationships between signal distribution methods, number of components, wire lengths, inherent errors and computation economics are derived and their trade-offs discussed. Although the relationships derived are applicable to an array of arbitrary size and shape, an example of a square 4000 element array is used in the conclusion to illustrate the application of these relationships.

---

\* Harrington, J. V., R. H. Baker and J. C. James: "Digitally Controlled Phased Array for Reception of Sunblazer Signals and Solar Radar Studies," M.I.T. Center for Space Research, TR-66-3.

## 1.0 POINTING EQUATIONS

Consider the vector  $\underline{N}$  pointing in the direction of wave propagation (i.e., normal to the plane wave front as shown in Figure A-1. When the wave front is coincident with point  $d_x$  on the x-axis, the distance from the wave front to the origin is  $N$ . This distance represents (in wave lengths) the relative phase between the point  $d_x$  and the origin. This phase expressed in radians is:

$$\phi_x = \frac{2\pi(N)}{\lambda} = \frac{2\pi}{\lambda} d_x \cos \rho_x \quad [1]$$

or in terms of the azimuth angle,  $\rho_{az}$ , and elevation angle,  $\rho_{el}$  (see Appendix A):

$$\rho_x = \frac{2\pi}{\lambda} d_x \cos \rho_{el} \cos \rho_{az} = \frac{\pi\sqrt{2}d}{\lambda} \cos \rho_{el} \cos \rho_{az} \quad [2]$$

And the phase between a point on the y axis,  $d_y$ , and the origin is:

$$\phi_y = \frac{2\pi}{\lambda} d_y \cos \rho_{el} \sin \rho_{az} = \frac{\pi\sqrt{2}d}{\lambda} \cos \rho_{el} \sin \rho_{az} \quad [3]$$

The quantities

$$\frac{\phi_x}{d_x} = \frac{2\pi}{\lambda} \cos \rho_{el} \cos \rho_{az} \quad [4]$$

$$\frac{\phi_y}{d_y} = \frac{2\pi}{\lambda} \cos \rho_{el} \sin \rho_{az} \quad [5]$$

are referred to as phase tapers and have the advantage that they have no dependence on the physical quantities of the antenna array.

## 2.0 DISTRIBUTION SCHEME

Figures 1A and 2A show possible envisioned arrays while 1B and 2B show these arrays rotated 45° to provide reduction in mathematical complexity. Envisioned signal paths\* are shown as a series of distribution nodes. Note that the total electrical distance to each dipole is the same.

If each node is considered to be in the center of a cell, the whole array can be thought of as a nested set of cells. It is convenient to define the number of subcells contained in any given cell as being the multiplicity,  $M$ , of the array.  $M$  is also the number or multiplicity of the branches stemming from each node. The total number of dipoles in the array then is  $N_D = M^L$  where  $L$  is the number of distributing points or nodes between any dipole and the outside world; and, therefore, is also the number of different levels of cells.

## 3.0 METHOD OF DISTRIBUTING PHASE CONTROL

It has been suggested that the phase imparted to each dipole be controlled through the use of phase shifters located at each node. Thus the phase of a particular dipole would be the total phase shift accumulated by the signal as it passes through all nodes between the receiver and the dipole.

$$\phi_{\text{dipole}} = \sum_{k=1}^L \phi_k \quad [6]$$

where  $k$  denotes the order of the node.

---

\* As suggested by R. H. Baker and staff.

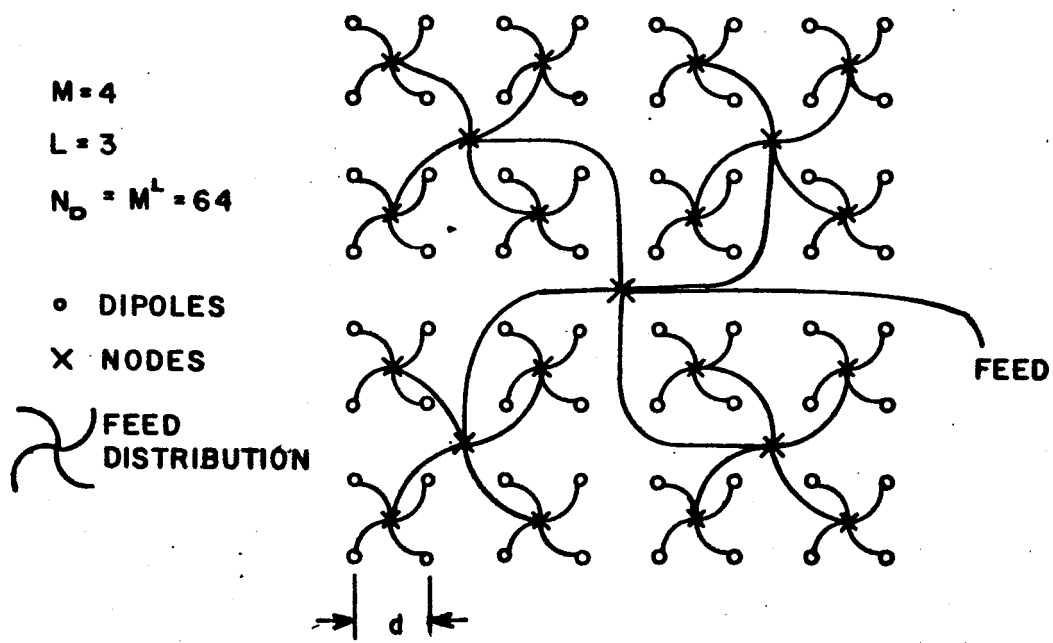


FIG. I-A

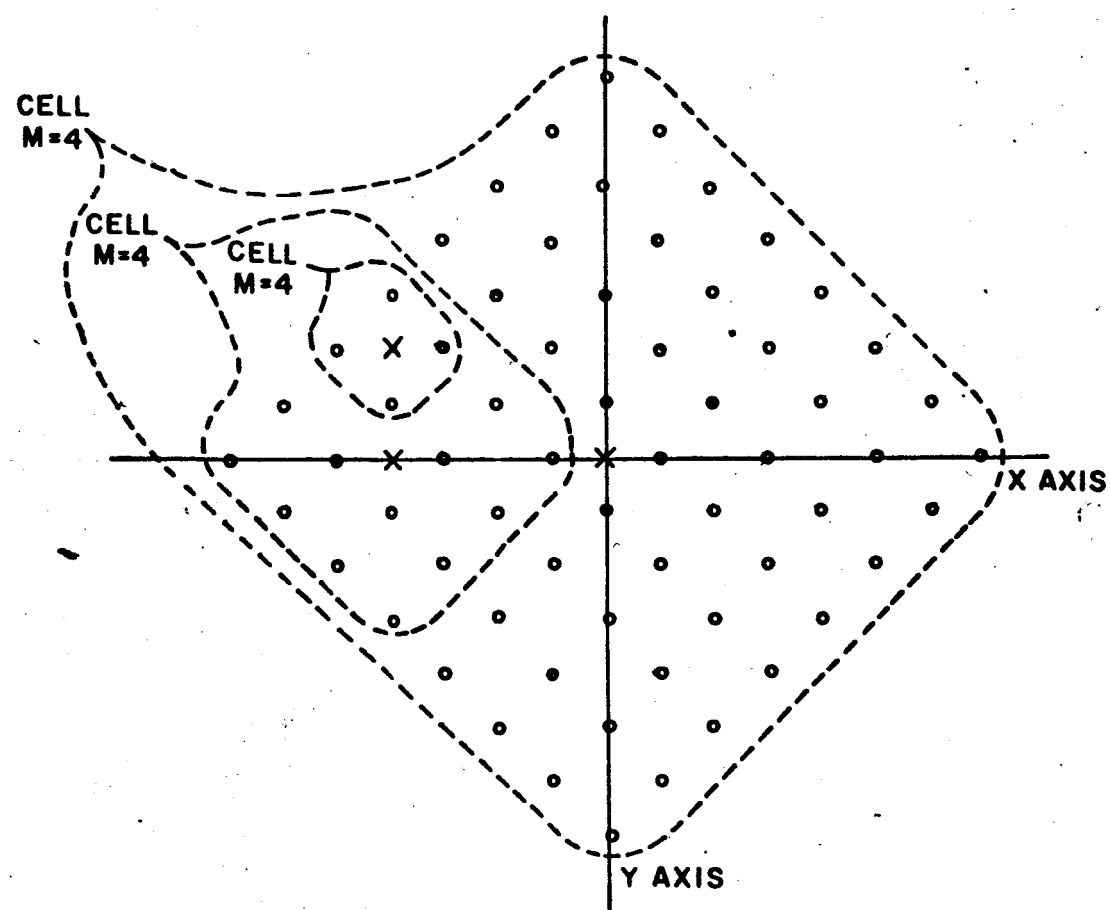


FIG. I-B

8 x 8 ANTENNA ARRAY

$M = 9$   
 $L = 2$   
 $N_o = M^L = 81$

◦ DIPOLES  
 \* NODES  
 (ALSO DIPOLE)

 FEED  
 DISTRIBUTION

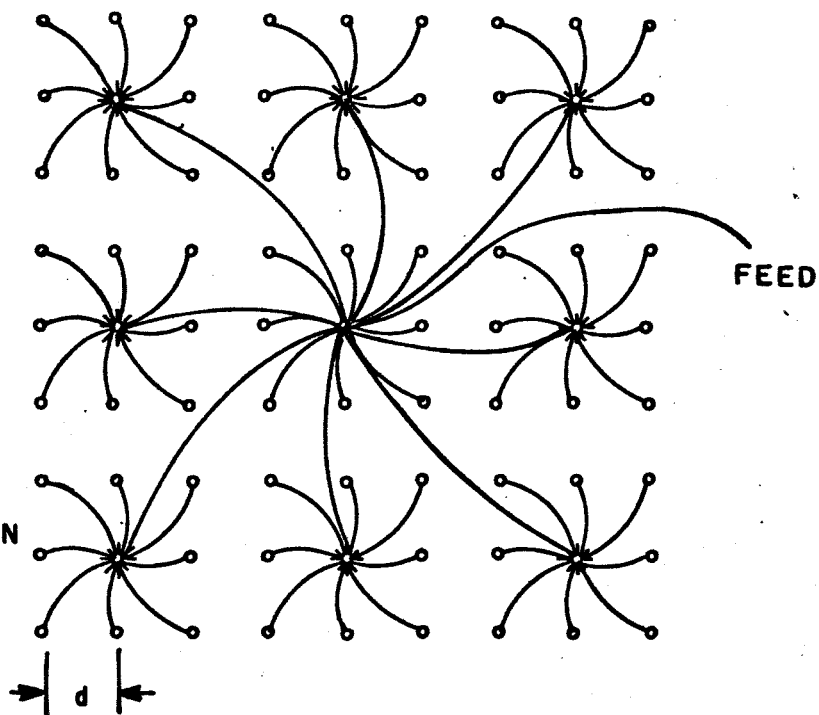


FIG. 2-A

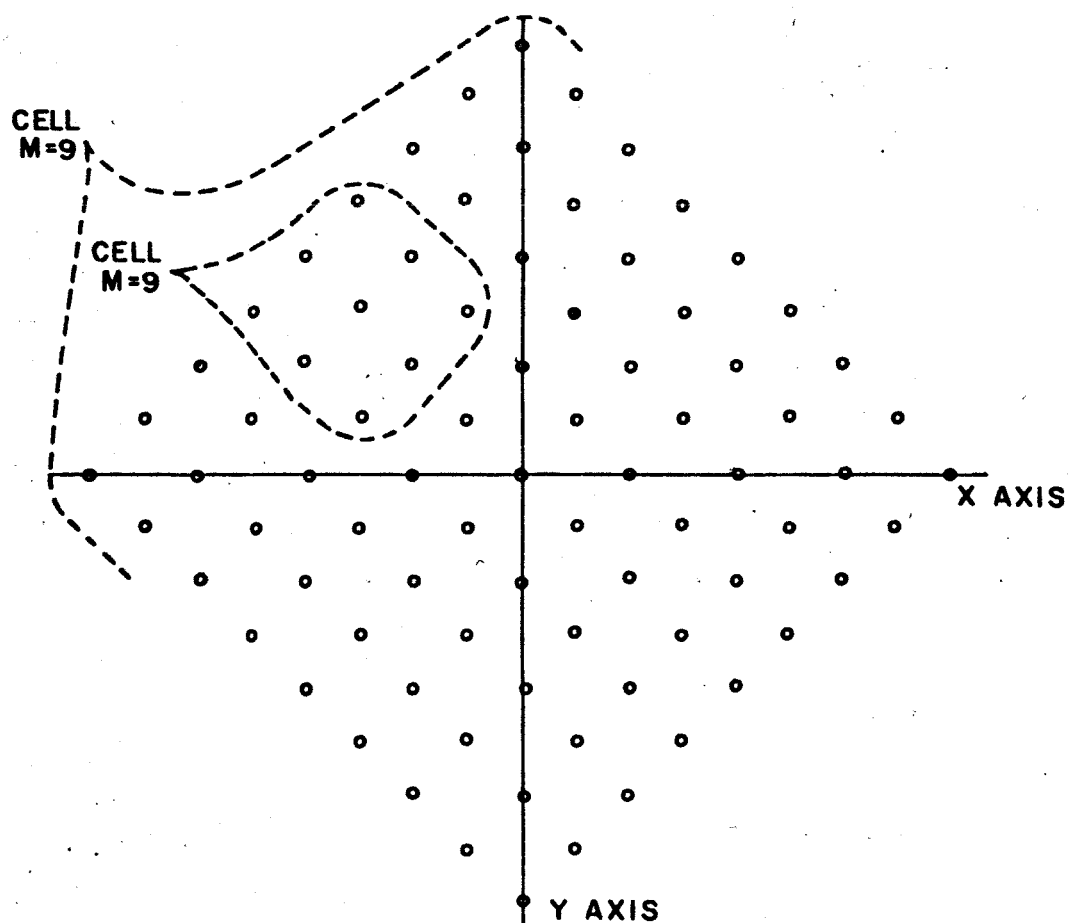


FIG. 2-B  
 9 x 9 ANTENNA ARRAY



It becomes convenient at this point to assume that the multiplicity is 4. If we assume the configuration in Figure 1B, then each phase shift occurs either in the x direction or y direction with opposing distributions from a node having opposite phase shifts. If we define a dipole location by the route a signal must take to reach it starting from the center of the array (first node), then we can express directly the phase of that dipole as a function of its location. Let us further define the direction embarked from a particular node as  $N = \frac{\text{angle}}{\pi/2}$ , i.e. for  $N=0$  along positive x axis,  $N=1$  along positive y axis,  $N=2$  along negative x axis, and  $N=3$  along negative y axis as shown in Figure 3A. Then the location of a particular dipole can be given by a series of numbers each of which can take on values from 0 to 3. Figure 3B gives an example for a 64 element array.

$D_{N_1, N_2 \dots N_k \dots N_L} = D_{2, 1, 0}$  = location of dipole in Figure 3B

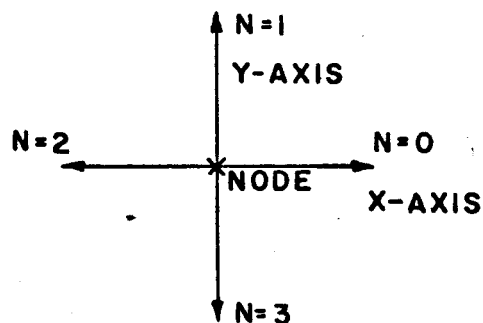
The relative phase at this dipole thus equals:

$$\text{Re} \left[ \sum_{k=1}^L 2^{L-k} (e^{j\pi N_k/2}) (\phi_x - j\phi_y) \right] = \phi_{\text{dipole}} \quad [7A]$$

or

$$\phi_{\text{dipole}} = \text{Re} \left[ \sum_{k=1}^L 2^{L-k+1} \frac{\pi d}{\lambda} e^{j\pi N_k} \cos \rho_{el} (\cos \rho_{az} - j \sin \rho_{az}) \right] \quad [7B]$$

$$= \frac{2^{L+1}}{\lambda} d \pi \cos \rho_{el} \sum_{k=1}^L 2^{-k} \text{Re} [e^{j(\rho_{az} - \pi N_k/2)}] \quad [7C]$$



$N_x = 0, 1, 2, \text{ or } 3$  SIGNIFIES NODE DEPARTURE

FIG. 3A

### NODE DEPARTURE

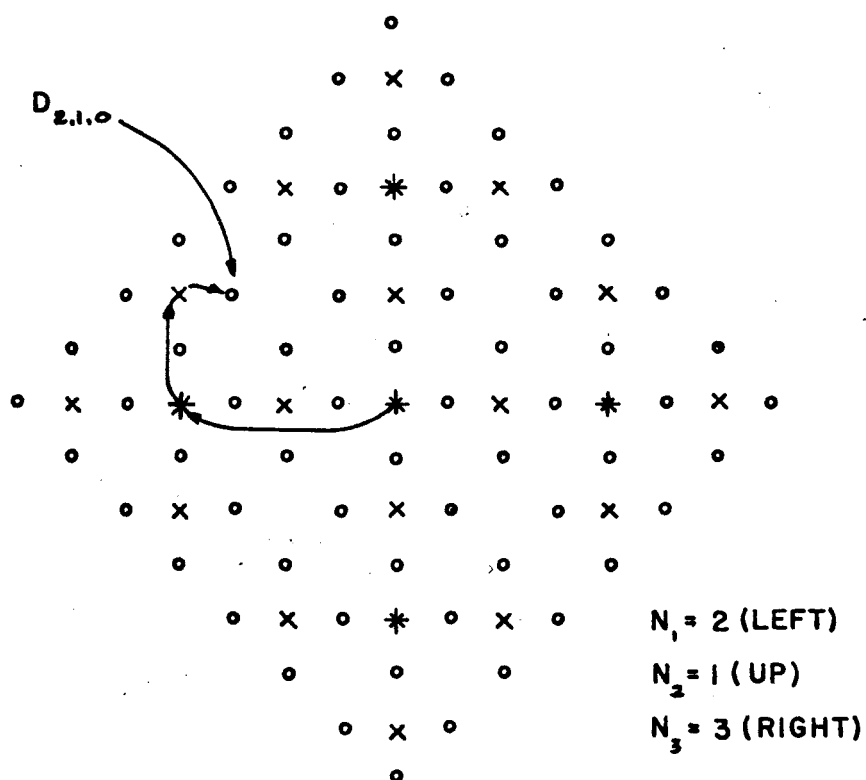


FIG. 3B

LOCATION OF DIPOLE BY NODE DIRECTION  
DESIGNATION

The above equation implies that only  $\rho_{az}$  and  $\rho_{el}$  need to be specified (i.e. the pointing angles) to control the phase at any dipole in the array. This equation also shows that the phase information supplied to each node is the same except for a factor of  $2^k$  depending on the cell level of the node. The values  $N_k$  for each node are merely the departing directions and are automatically hard-wired into each node.

Thus if the two magnitude values of the expression in [7C] ( $N_k = \text{even}$ ,  $N_k = \text{odd}$ ) are expressed as binary words and the phase shifters are linear, then only these two words need be supplied to the nodes to control the phase distribution of the entire array. The only calculations needed for different node levels are binary shifts (i.e. division by two). Even if the multiplicity distribution scheme (Figure 1A) is not used, [7C] is still useful in that a distribution computer only needs to solve this equation to direct the array.

#### 4.0 QUANTIZATION

If we were using continuous phase shifters, the relative phase of each dipole could be controlled exactly (within engineering tolerances). However, economical considerations indicate that quantized phase shifters might be more practical. It is the purpose of this section to explore some of the implications and restrictions imposed through the use of quantized phase shifters.

Let the following binary word be a typical phase shift word of infinite resolution:

0011.010111:01001 . . .  $2\pi(3.3643 . . .)$   
 $\wedge \quad \wedge$   
 1st bit qth bit

where those bits to the left of the period denote a number of " $2\pi$ " phase shifts and those bits to the right denote that portion of the phase shift less than  $2\pi$ . The ":" denotes the point of quantization. The LSB (least significant bit) above the quantization shall be referred to as bit  $q$ , i.e. the LSB carries  $2\pi \times 2^{-q}$  phase angle.

The bits prior to the period can be ignored at each phase shifter in that we are working with a modular  $2\pi$  system. The bits following ":" will be referred to as the residue.

If the desired pointing angle has a non-zero residue, then quantization will introduce a quantizing error dependent on the residue. The maximum peak error at the worst case dipole due to quantization is discussed in the following two sections in that it is akin to a tolerance in an antenna dish and also because it can be readily calculated.

In 4.1 and 4.2 it is assumed that the proper phase shift word is supplied to each node and the quantization at one node does not alter the word supplied to the other nodes.

#### 4.1 TRUNCATION

The first and perhaps easiest form of quantization is truncation, i.e. just ignoring the bits below the quantization

level  $q$ . Truncation would result in the largest possible error at any dipole approaching  $2\pi \times 2^{-q} \times L$ . Normalizing this error by the LSB, i.e.  $2\pi \times 2^{-q}$ , this maximum error approaches  $L$  (see Appendix B for detailed discussion).

#### 4.2 ROUNDING OFF

Rounding off prior to truncation improves (reduces) the peak error due to quantization. The improvement factor approaches  $2^{\frac{1}{2}}$  for  $M=4$  and is equal to 2 for all odd  $M$  or large even  $M$  (see Appendix B). This improvement is significant enough to warrant rounding off prior to all truncation.

A detailed discussion of the quantization errors due to rounding off is given in Appendix B. It is worthwhile noting, however, that the peak error for a very large array can always be reduced by increasing  $M$  in that the effect of a reduction of nodes more than offsets the improvement factor advantage of  $M=4$ .

#### 4.3 QUANTIZING THE LOOK ANGLES

If the pointing directions are quantized such that [8] is forced to hold for any integer value of  $P$  (see [7C],

$$\frac{\pi d}{\lambda \sqrt{2}} \cos \rho_{el} \operatorname{Re} [e^{j(\rho_{az} + \pi N_k/2)}] = 2^{-q} \times 2\pi P \quad [8]$$

$$P = 0, 1, 2, \dots$$

then the residue in the phase shift words will be zero at all nodes and no quantization error will exist; however, a pointing

error will exist. If the loss in overall gain due to incorrect pointing is greater than it would be due to the presence of unfavorable residues (lack of smoothness in the phase taper approximation), then a pointing quantization should not be employed to the full extent.

Figure 4 shows the most favorable ( $M=N_D$ ) quantized look angles for  $q=4$  (i.e. phase angles quantized in  $\frac{2\pi d}{\lambda} (\frac{1}{16})$  increments). Note that even looking straight up, the worst pointing error due to pointing quantization is  $\frac{3.6}{\sqrt{2}} = 2.5^\circ$ . Thus even for a beam width as wide as  $5^\circ$ , this point would be 3 db down. For  $M=4$  there is further spread of these look angles of  $\sqrt{2}$ , making the main pointing error equal to  $3.6^\circ$ .

By allowing some pointing error and some quantizing error, in the section 4.2 sense, an optimum distribution scheme can be achieved. This optimum would quantize the look angles in smaller increments than  $2\pi \times 2^{-q}$  and allow only those residues that would contribute quantizing error to the last few nodes.

Now increasing  $q$  has a very strong effect on the improvement of both types of errors. However, computation costs and distribution costs would increase with  $q$  so that  $q$  should be held to as small a value as is practical with respect to errors. The procedure for calculating the smallest allowable value of  $q$  is involved but not difficult and depends on the size of the array. In general, a larger array means a narrower beam width, and thus a larger value of  $q$  is necessary to keep the overall

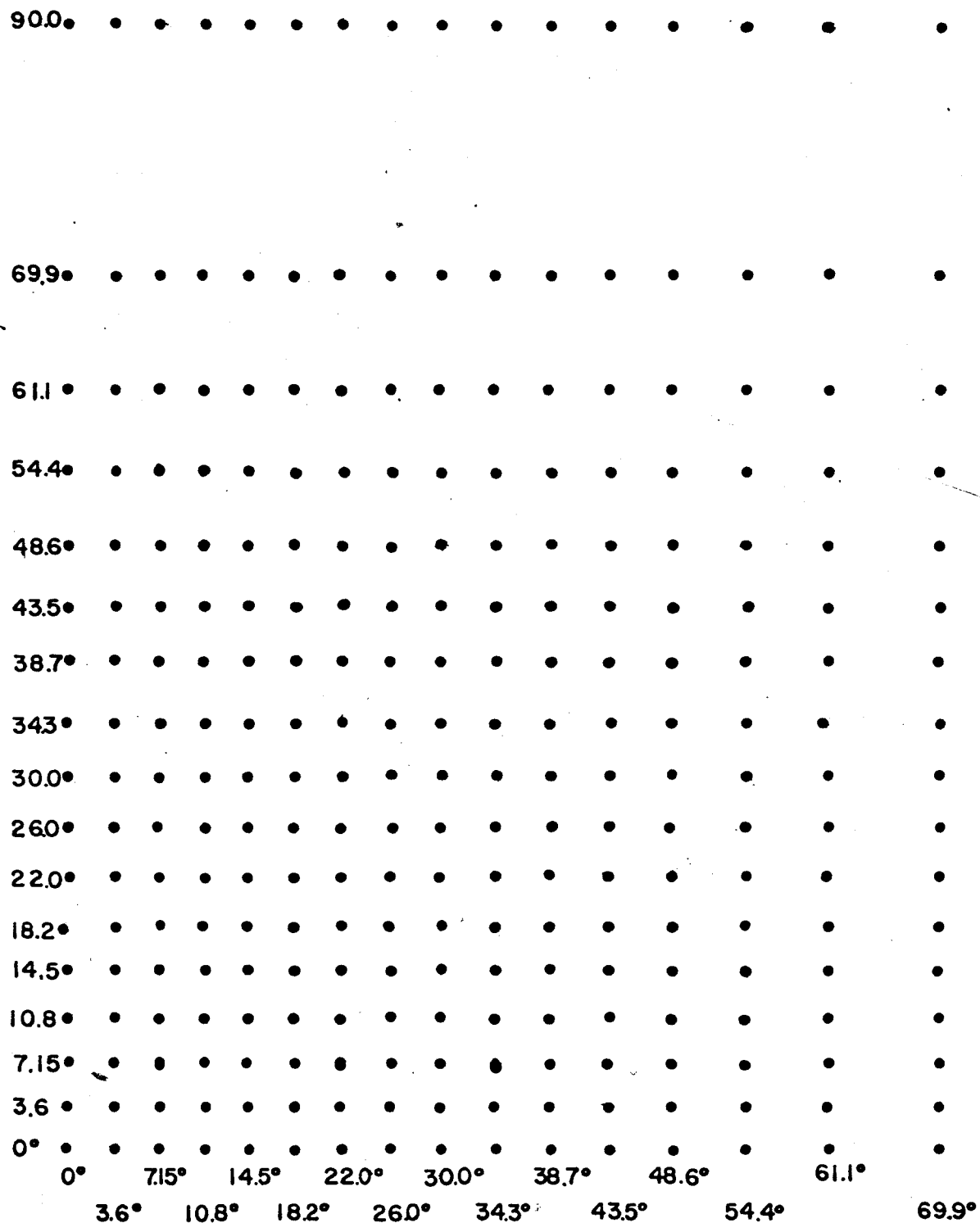


FIG. 4  
 QUANTIZED LOOK ANGLES  
 for  $M = N_D$  (most favorable)  $q = 4$

errors within tolerance. Therefore, the computational costs increase at a faster rate than the array size.

## 5.0 ECONOMICS

In choosing a distribution system it becomes important to consider the different cost aspects to arrive at some optimum criterion. The factors considered here are:

1. Number of phase shifters per dipole
2. Wire length
3. Computation costs

### 5.1 PHASE SHIFTERS PER DIPOLE

Assuming again that the phase shifter can add both a positive phase increment and a negative phase increment, we can proceed to calculate the number of phase shifters per dipole as a factor of M and L (without this assumption multiply  $N_p$  by 2).

Thinking of the phase distributing method for a moment, it is not difficult to see that the number of phase shifters for M=even can be expressed as:

$$N_p = \frac{N_D}{2} + \frac{N_D}{2M} + \frac{N_D}{2M^2} \cdot \cdot \cdot \frac{N_D}{2M^{L-1}} = \frac{1}{2} \frac{M}{M-1} [N_D^{-1}] \quad [9]$$

and for M=odd:

$$N_p = \frac{N_D}{2} \left[ \frac{M-1}{M} \right] + \frac{N_D}{2} \left[ \frac{M-1}{M^2} \right] + \frac{N_D}{2} \left[ \frac{M-1}{M^3} \right] \cdot \cdot \cdot = \frac{N_D^{-1}}{2} \quad [10]$$

A plot of  $\frac{N_p}{[N_D^{-1}]}$  for some values of M is shown in Figure 5.



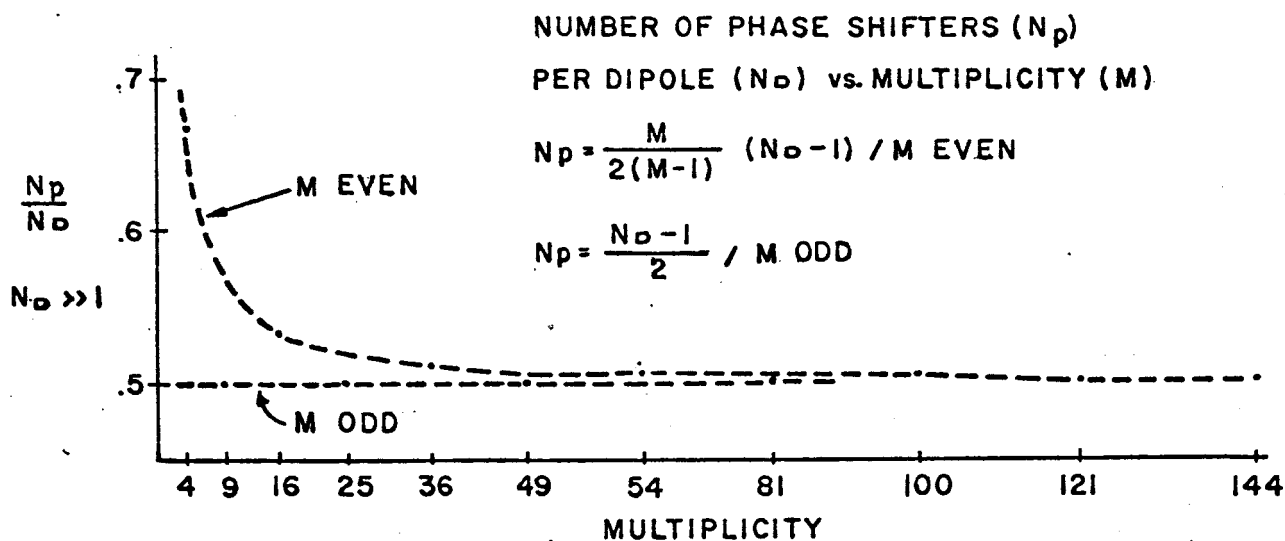


FIG.5

### NUMBER OF PHASE SHIFTERS PER DIPOLE

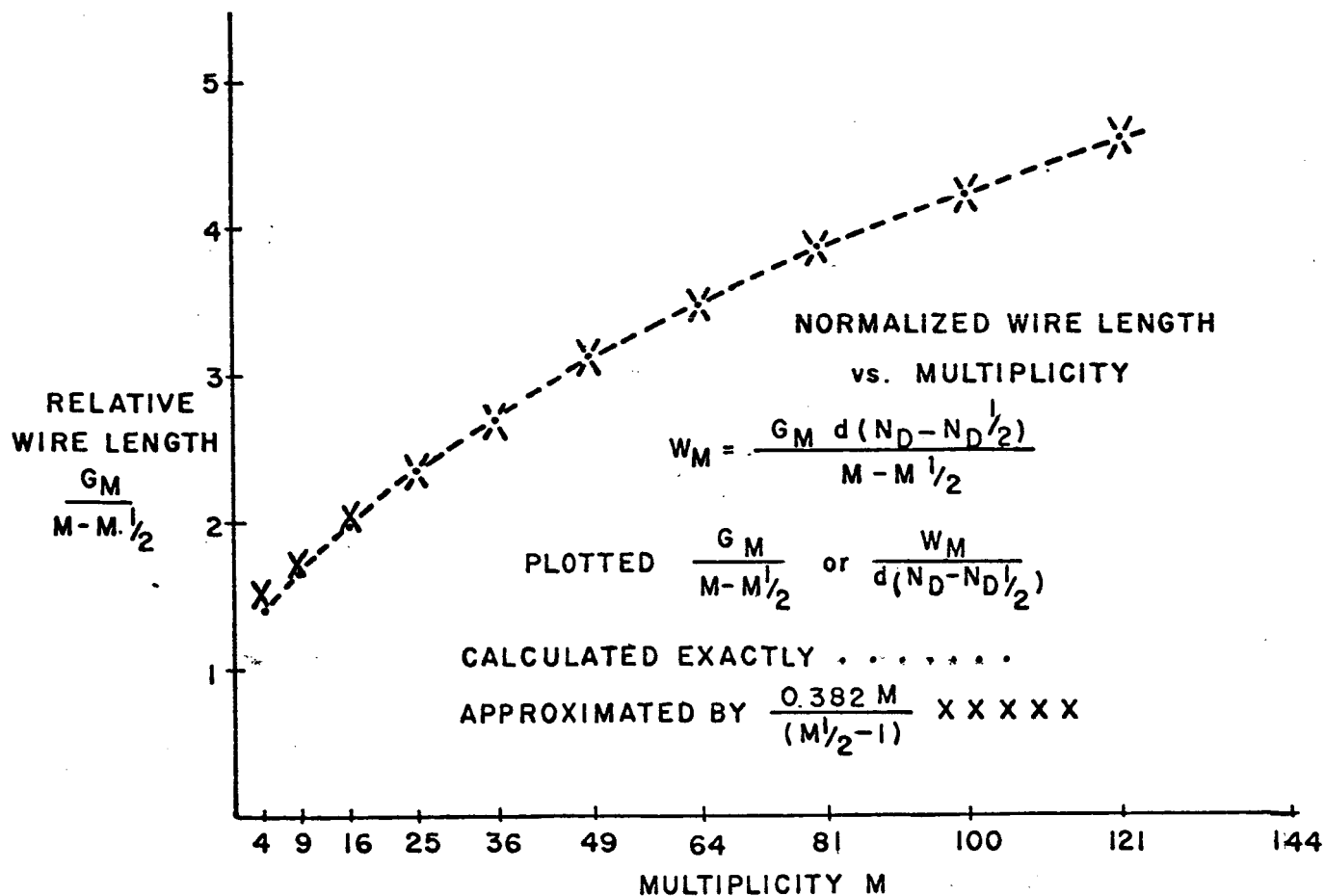


FIG.6

### NORMALIZED WIRE LENGTH vs. MULTIPLICITY

Note that only for  $M=4$  or  $M=16$  is there much added cost with regard to phase shifters using the multiplicity distribution approach.

## 5.2 WIRE LENGTH

Wire length is a real consideration in that, for such a large number of dipoles, wire length can contribute significantly to the overall cost. If it is assumed that all distributions are initiated from the geometric center of the array, then it is possible to express the total wire needed as a function of  $M$  and  $N_D$  (see Appendix C). The results of Appendix C are shown in Figure 6. Note that for  $N_D = 64$  a saving factor of  $2^{\frac{1}{2}}$  in total wire length can be realized by setting  $M=4$  instead of  $M=64$ . The savings with  $M=4$  for an arbitrarily large array is approximately:

$$\frac{W_{N_D}}{W_4} = \frac{0.38 N_D^{\frac{3}{2}}}{\sqrt{2d(N_D - N_D^{\frac{1}{2}})}} \approx 0.3 N_D^{\frac{1}{2}} \quad [11]$$

For  $N_D = 2^{12} = 4096$  this saving in total wire length is nearly a factor of 20.

The general expression for the wire saving as a function of  $M$  and  $N_D$  is given in Appendix C.3 [C-8].

## 5.3 COMPUTER COSTS

A cell of arbitrary  $M$  can be thought of as composed of a superposition of ( $M=4$ ) subcells as shown in Figure 7. The only differences between each of the  $M=4$  subcells are a scale

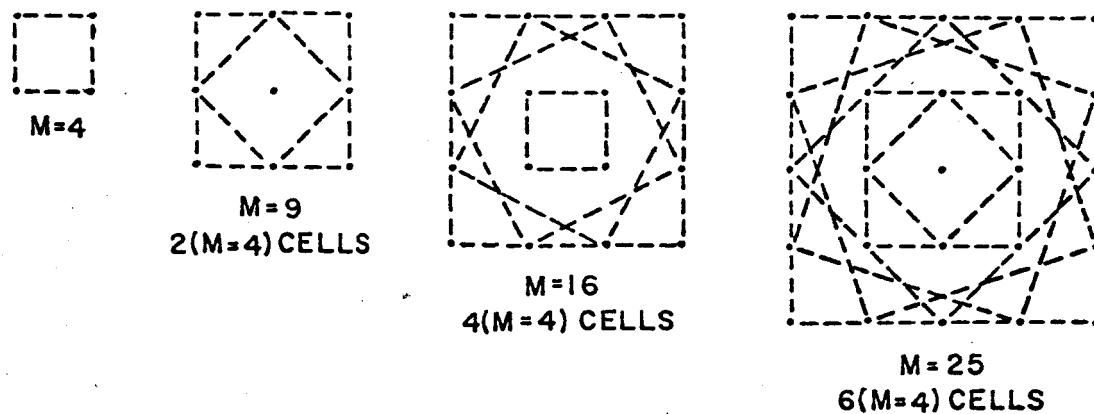


FIG. 7

SUPERPOSITION OF M=4 CELLS FOR CONSTRUCTION OF ARBITRARY M CELL

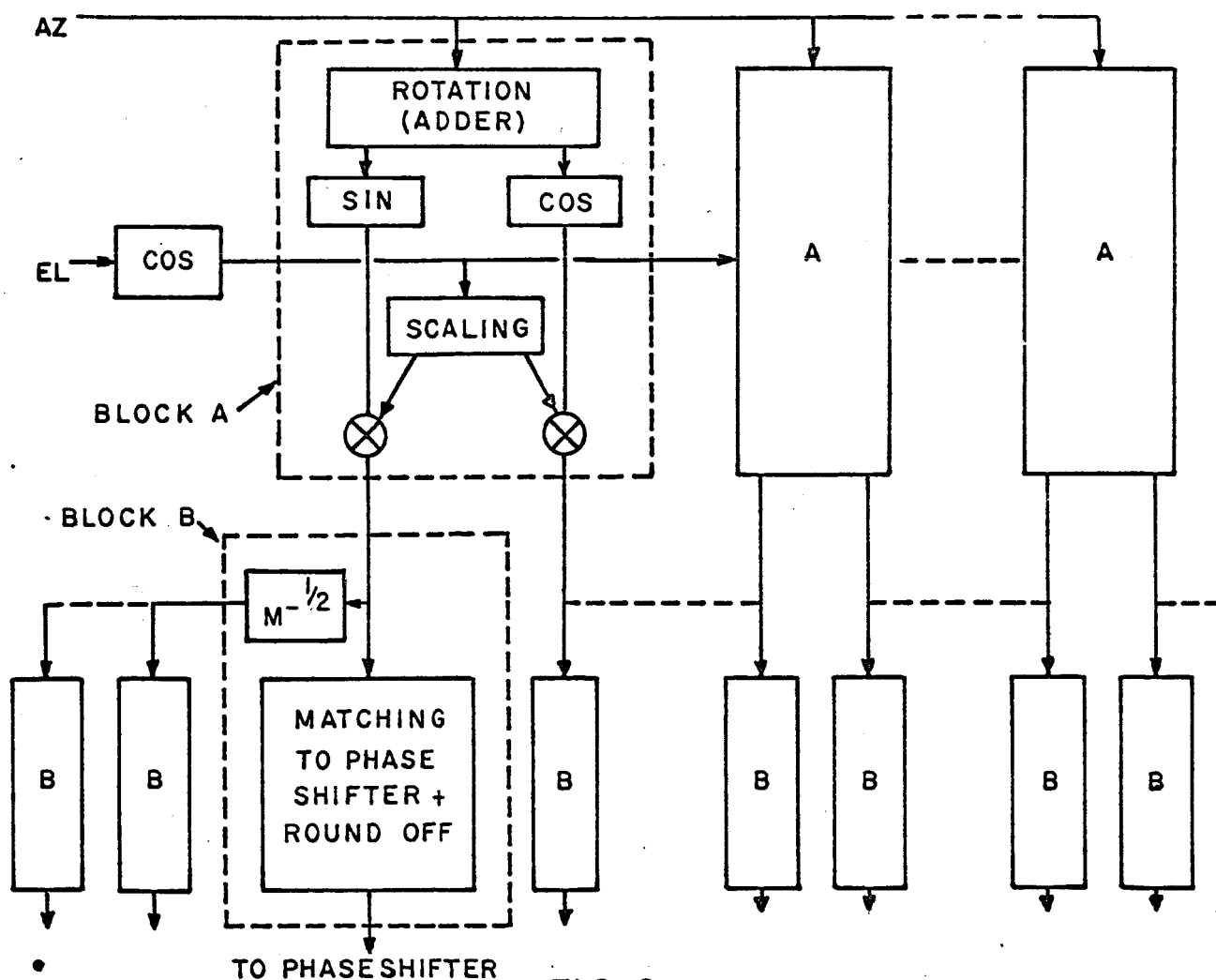
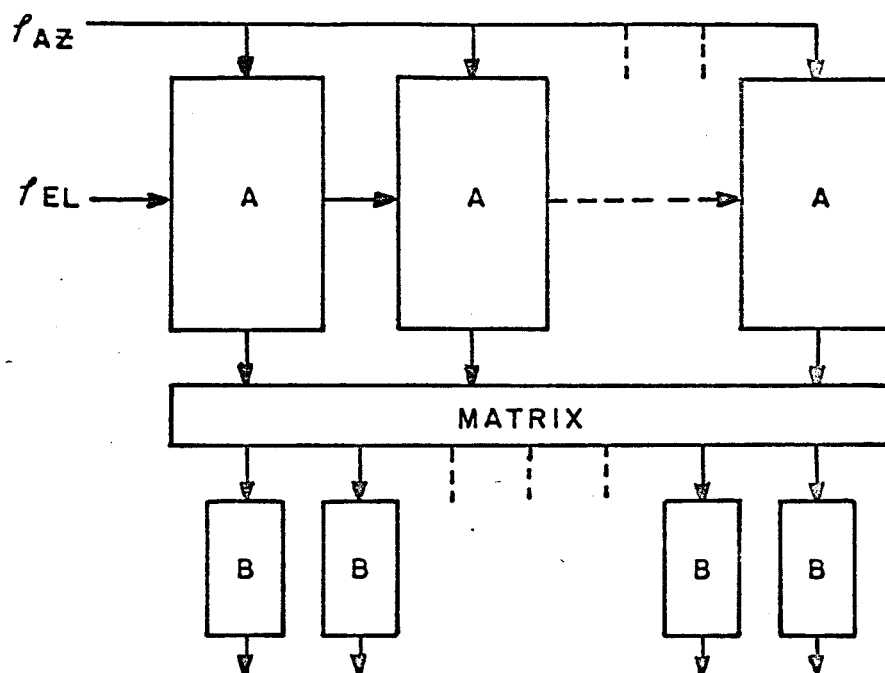


FIG. 8

COMPUTER BLOCK DIAGRAM

factor and a rotation. The computer block in Figure 8 shows how the phase word can be computed for any one of the  $M=4$  subcells. Since a cell can be broken down into  $\frac{M}{4} (\frac{M-1}{4})$  if  $M$  is odd) subcells and each subcell needs two words, the total number of phase shift words that have to be generated is  $\frac{ML}{2} (\frac{(M-1)L}{2})$  for odd  $M$ ) or  $\frac{M \ln N_D}{2 \ln M}$  words for the entire array. This means that  $\frac{M}{4}$  block A's and  $\frac{M \ln N_D}{2 \ln M}$  block B's must be constructed. Fortunately, block A is the more expensive of the two block types in that it contains sin and cos generators along with some adders and multipliers. If the phase shifters are linear, then blocks B are of low cost in that each word is related to the output of block A by a small multiple ( $M^{\frac{1}{2}}$ ). If  $M$  is a power of 2, then the cost is effectively zero in that the outputs can be taken from the same word with only a difference in the wiring. Non-linear phase shifters should be avoided unless the increased cost of block B (of which there are many) is compensated for by a saving in the cost of the phase shifters.

If a multiplicity is a power of a lower multiplicity (i.e. 16, 64, 81, 125, etc.), then a variation in the aforementioned computer can result in considerable savings. Figure 9 illustrates this point. Now the outputs of blocks A can be added to yield the phase shift words. Thus the number of A blocks (with  $M=M_S^P$ ) becomes  $\frac{M_S}{4} (\frac{M_S-1}{4})$  for  $M_S$  odd) resulting in considerable saving of complexity and cost. The number of B blocks remains unchanged. If, in addition  $M_S = 4$ , i.e.  $M = 4^P$ , then



SAVINGS  
IN A BLOCKS  
of  $\frac{M}{M_s K}$

$M = 9, 25, 36, 49, \dots$

$$K = \frac{L_n M}{L_n M_s}$$

FIG. 9

COMPUTER BLOCK DIAGRAM FOR  $M = M_s^K$

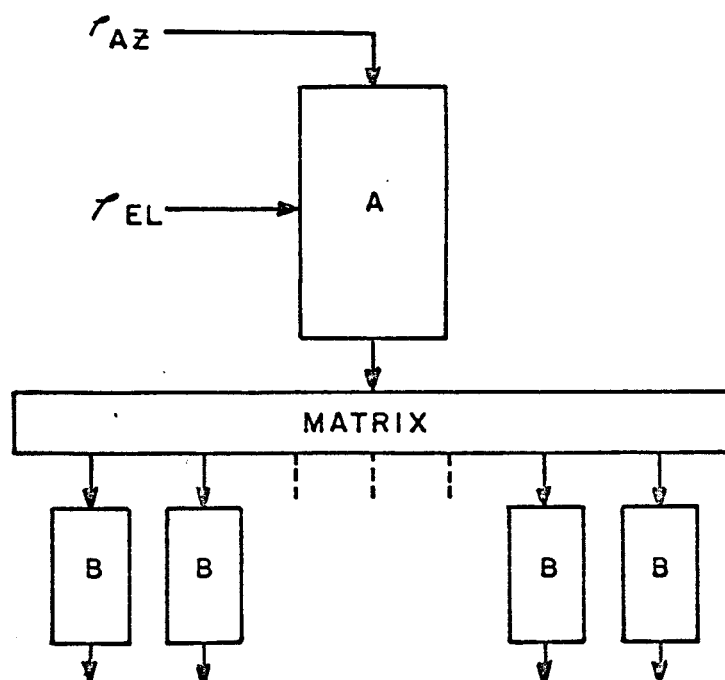


FIG. 10

COMPUTER BLOCK DIAGRAM FOR  $M = M_s^K$  AND  $M_s = 4$

only a single block A is needed with shifters replacing the other A blocks (Figure 10).

It is interesting to note that even if one were to set  $M = N_D = M_s^L$  and thus not use the multiplicity concept in the distribution, the multiplicity concept is still very important to the efficient realization of the computer.

## 6.0 SUMMARY

There are definite advantages associated with both large multiplicities and small multiplicities. The advantages of large multiplicities are: less quantization error (smaller value of L), fewer phase shifters, more central control (phase shifts more concentrated) and the advantage of fewer connections and less electrical distance between a dipole and the receiver. On the other hand, small multiplicities have the advantage of less total wire length and a simpler and cheaper computer which in turn implies easier control.

The final choice is dictated by the geometry and number of dipoles. For example, if the array is small, wire length ceases to be a consideration.

### 6.1 LET $N_D = 2^{12}$ OR 4,000 DIPOLES

The consideration of a particular example will illustrate some of the trade offs encountered in the choice of M. For  $N_D = 2^{12}$ , a good choice of parameters would be  $M=16$  and  $L=3$ . These choices make for a simple computer (since  $M_s^2 = M$  where

$M_s = 4$ ) near minimum wire length (40 percent more than  $M=4$  but only about  $\frac{1}{12}$  the wire length for  $M=2^{12}$ ), only about 15 percent more phase shifters than optimum, and a controllable quantization error. I would use  $q=4$  (four bits to control phase shifter) for the last phase shift distribution ( $\frac{\lambda}{32}$  maximum error, 2,000 phase shifters);  $q=5$  (five bits control) for the middle phase shifter distribution ( $\frac{\lambda}{64}$  maximum error, 128 phase shifters) and  $q>6$  (six or more bit control) for the first set of 8 phase shifters. This distribution scheme would make the total maximum error due to quantization less than  $\frac{\lambda}{16}$  while enabling pointing angle resolution to better than a minute of arc.

# APPENDIX A

## DERIVATION OF RELATIONSHIPS BETWEEN $\rho_x$ , $\rho_y$ , AND $\rho_{az}$ , $\rho_{el}$ (Figure A)

From the law of cos:

$$N^2 (\sin^2 \rho_{el} + \cos^2 \rho_{el} \tan^2 \rho_{az}) = N^2 + \frac{N^2 \cos^2 \rho_{el}}{\cos^2 \rho_{az}} - \frac{2N \cos^2 \rho_{el}}{\cos^2 \rho_{az}} \cos \rho_x$$

$$\cos \rho_{az} = \frac{1}{2} \frac{\cos \rho_{el}}{\cos \rho_{az}} - \frac{1}{2} \frac{\sin \rho_{el}}{\cos \rho_{el}} \cos \rho_{az} + \cos \rho_{el} \frac{\sin^2 \rho_{az}}{\cos \rho_{az}} + \frac{1}{2} \frac{\cos \rho_{az}}{\cos \rho_{el}}$$

$$= \frac{1}{2} \frac{\cos \rho_{el}}{\cos \rho_{az}} (1 - \sin^2 \rho_{az}) + \frac{1}{2} \frac{\cos \rho_{az}}{\cos \rho_{el}} (1 - \sin^2 \rho_{el})$$

$$= \frac{1}{2} \frac{\cos \rho_{el}}{\cos \rho_{az}} (\cos^2 \rho_{az}) + \frac{1}{2} \frac{\cos \rho_{az}}{\cos \rho_{el}} (\cos^2 \rho_{el}) = \cos \rho_{el} \cos \rho_{az}$$

$$\text{also: } \cos \rho_p = \cos \rho_{el} \cos (90^\circ - \rho_{az}) = \cos \rho_{el} \sin \rho_{az}$$

Therefore, the relationships between  $\rho_x$ ,  $\rho_y$ ,  $\rho_{el}$ , and  $\rho_{az}$  are:

$$\cos \rho_x = \cos \rho_{el} \cos \rho_{az} \quad [A-1]$$

$$\cos \rho_y = \cos \rho_{el} \sin \rho_{az} \quad [A-2]$$





## APPENDIX B

### ERRORS DUE TO QUANTIZATION

As a signal passes through a node towards a dipole, its phase is changed by either a positive or negative increment. Since signals distributed through opposite branches are changed by increments identical in magnitude but opposite in sign, it is always possible to follow a signal accumulating only positive increments on its way to a radiating dipole. The error at the worst case dipole for any arbitrary pointing angle is therefore just the sum of the magnitudes of the errors accumulated at each node. Since only that portion of the pointing angle eliminated by quantization (i.e. the residue) contributes to the error, it is sufficient to study the error as a function of this residue normalized by the quantization level.

Figure B-1A shows the relationship between the worst case normalized dipole error and the normalized residue for a single cell ( $L=1$ ) and  $M=4$  with pure truncation. Here the error is merely the residue per se. Figure B-1B shows the resulting error when  $L$  is extended to 2. Note that this is just a superposition of B-1A and a double term denoting the additional error contributed by a second node. The remaining B-1 figures show what happens as  $L$  increases further. The maximum total error is reached when the normalized residue is just short of 1 and in effect is equal to  $L$  as would be expected.

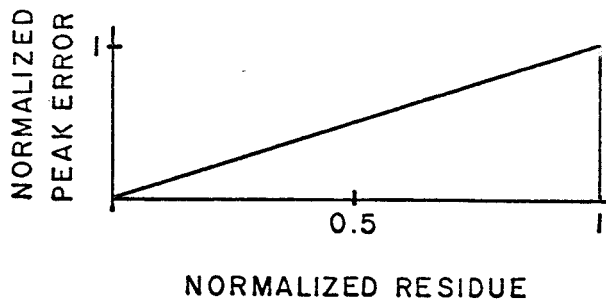


FIG. B-1A  $L=1, M=4$

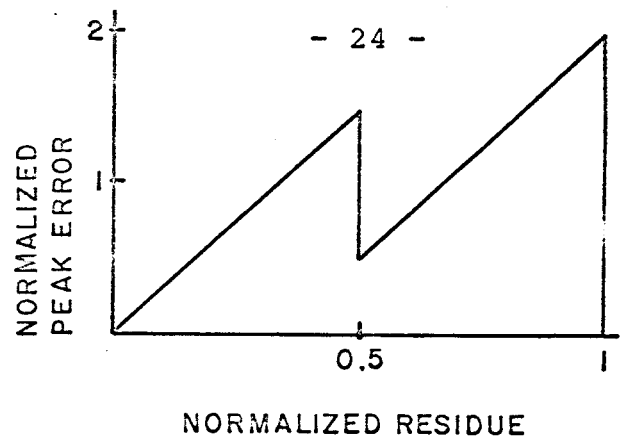


FIG. B-1B  $L=2, M=4$

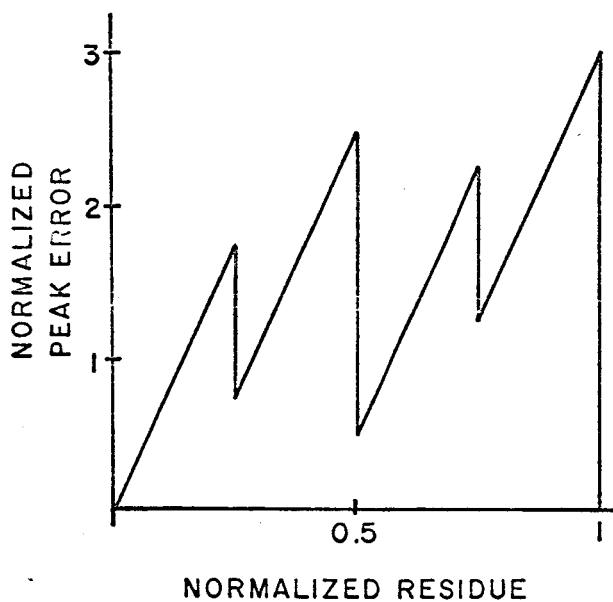


FIG. B-1C  $L=3, M=4$

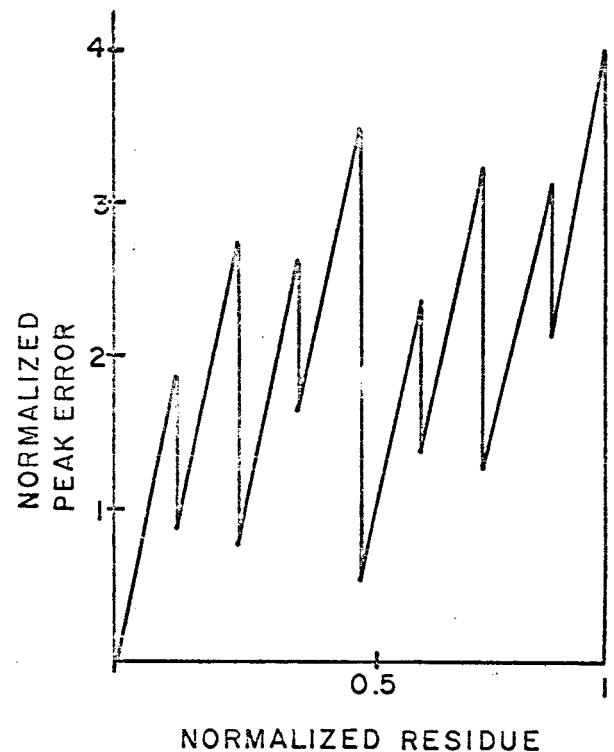
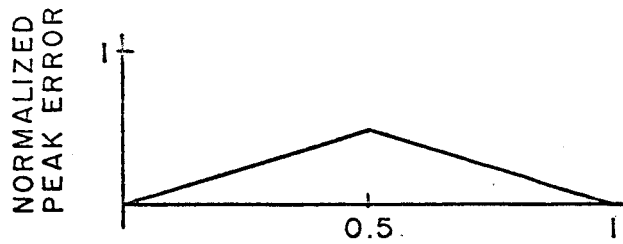


FIG. B-1D  $L=4, M=4$

FIG. B-1

PEAK ERROR AT WORST CASE DIPOLE (DUE TO QUANTIZATION)  
WITH PURE TRUNCATION (AS A FUNCTION OF THE NORMALIZED  
RESIDUE)



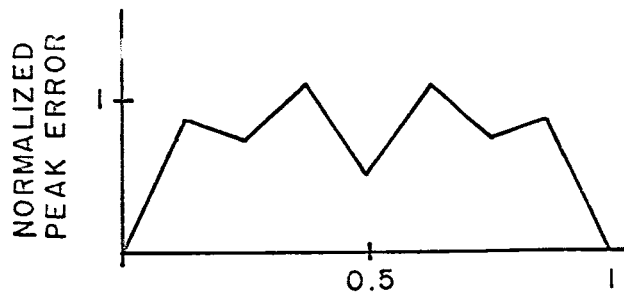
NORMALIZED RESIDUE

FIG. B-2A  $L=1, M=4$



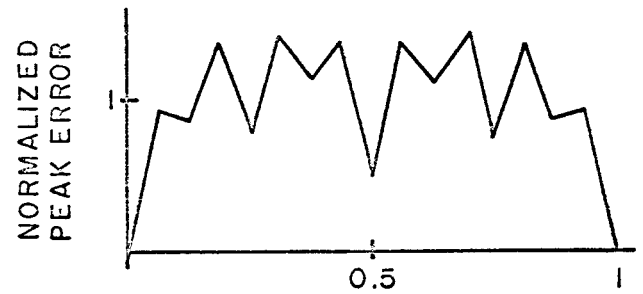
NORMALIZED RESIDUE

FIG. B-2B  $L=2, M=4$



NORMALIZED RESIDUE

FIG. B-2C  $L=3, M=4$



NORMALIZED RESIDUE

FIG. B-2D  $L=4, M=4$

FIG. B-2

PEAK ERROR AT WORST CASE DIPOLE (DUE TO QUANTIZATION)  
WITH ROUNDING OFF (PRIOR TO TRUNCATION AS A FUNCTION  
OF THE NORMALIZED RESIDUE)

(ALONG X AXIS OR Y AXIS)

Figure B2-A shows the effect on the error as a result of rounding off prior to truncation for  $L=1$ . As expected, the peak value is  $\frac{1}{2}$ . Figure B2-B shows the maximum error along either the x-axis or y-axis for  $L=2$ . As in the case of Figure B1-B, this figure is a superposition of Figure B2-A and a double error term resulting from the second node. This double term does not peak where the first error does. The peak error is not  $2 \times \frac{1}{2} = 1$ , therefore, but rather  $\frac{1}{2} + \frac{1}{4} = \frac{3}{4}$ . Figures B2-C, etc. show this error for larger values of  $L$ . It is interesting to note that, for larger values of  $L$ , the total error approaches  $\frac{1}{3} \times L$  and not  $\frac{1}{2} \times L$  as might be expected. The improvement then along the axes resulting from rounding off prior to truncation is a factor of 3.

The off-axis errors are larger than the on-axis errors in that the x-axis residues and y-axis residues are uncorrelated. The worst possible case is generated by alternating axes, i.e. as close to the  $45^\circ$  diagonal as the discreteness of the array will allow. For large  $L$  and  $M=4$ , the diagonal error approaches  $0.4 \times L$  which is a factor of  $2\frac{1}{2}$  improvement over pure truncation.

For  $M=9$  the worst case peak errors occur along the axis. The total error is again found by a superposition of the errors contributed at each node. Since all the contributions peak for the same residue, this is the maximum peak error which an off-axis cannot exceed. For  $M=25, 49 \dots$  the maximum peak errors

will also occur along the axis and each node will contribute an error of 0.5 for a total maximum peak error of 0.5L.

For  $M=16$  very little cross correlation remains between the error terms, and thus the diagonal maximum peak error is almost 0.5L (actual 0.47L). For  $M=36, 64, 100 \dots$  the maximum peak errors are also along the diagonals and are effectively 0.5L.

# APPENDIX C

## CALCULATION OF WIRE LENGTHS VERSUS M AND $N_D$

Let us define the wire length in the small cell of multiplicity M as  $G_M d$  (where d is the dipole spacing and  $G_M$  is a geometric constant depending on M). Then the contribution to the total wire length due to all of the small cells is  $\frac{dG_M N_D}{M}$  and the total wire length can be expressed in a series where each term is the contribution due to those cells at a particular level.

$$W_M = \frac{dG_M N_D}{M} \left[ 1 + \left(\frac{1}{M}\right)^{\frac{1}{2}} + \left(\frac{1}{M^2}\right)^{\frac{1}{2}} + \left(\frac{1}{M^3}\right)^{\frac{1}{2}} \dots \left(\frac{1}{M^{L-1}}\right)^{\frac{1}{2}} \right] \quad [C-1]$$

or

$$W_M = \frac{dG_M (N_D - N_D^{\frac{1}{2}})}{M - M^{\frac{1}{2}}} \quad [C-2]$$

or normalizing by all terms which do not depend on the distribution method:

$$\frac{W_M}{d(N_D - N_D^{\frac{1}{2}})} = \frac{G_M}{M - M^{\frac{1}{2}}} \quad [C-3]$$

# C.1 $W_M$ FOR $M = N_D$ FOR LARGE ARRAYS

An approximation to the total wire length with  $M=N_D$  for large arrays can be calculated by multiplying the densities of dipoles,  $\rho$ , in a delta area weighted by the wire length to the middle of the array and then integrating over the entire array.

$$\begin{aligned}
 W_{N_D} \Big|_{N_D \rightarrow \infty} &= \int \int_A \rho r dA = \frac{8}{d^2} \int_0^{\frac{\pi}{2}} d\theta \int_0^{N_D^{\frac{1}{2}} d(\frac{1}{2 \cos \theta})} r^2 dr \\
 &= \frac{dN_D^{\frac{3}{2}}}{3} \int_0^{\frac{\pi}{4}} \frac{d\theta}{\cos^3 \theta} = \frac{dN_D^{\frac{3}{2}}}{6} \left[ \sqrt{2} + \int_0^{\frac{\pi}{4}} \frac{d\theta}{\cos \theta} \right] \quad [C-4]
 \end{aligned}$$

or

$$W_{N_D} \Big|_{N_D \rightarrow \infty} = 0.382 dN_D^{\frac{3}{2}} \quad [C-5]$$

The significance of this result is that  $W_{N_D}$  increases as  $N_D^{\frac{3}{2}}$  where, if  $M$  is held to some constant value,  $W_M$  increases linearly with  $N_D$ . Thus for large arrays a considerable savings in wire length and therefore cost can be accomplished by holding  $M$  to some constant value (i.e. 4, 9, etc.)



## C.2 $W_M$ FOR ARBITRARY VALUES OF M

It is of interest to compare [C-5] with [C-2] to see how large the array must be to make [C-5] valid. Exact calculated values for  $G_M/(M-M^{\frac{1}{2}})$  for  $M=4, 9, \dots$  are plotted against M in Figure 6, page 14, as a series of dots.  $G_M(M-M^{\frac{1}{2}})$  as calculated by combining [C-5] and [C-3] is shown in Figure 6 as a series of X's and are given in [C-6].

$$\frac{G_M}{M-M^{\frac{1}{2}}} \approx 0.382 \frac{M}{M^{\frac{1}{2}}-1} \quad [C-6]$$

The approximation is quite good for all but the lowest values of M. It is worthwhile then to substitute [C-6] into [C-3] to obtain an equation for  $W_M$  dependent entirely on known quantities. The resulting approximation is within two percent for M greater than 9 and within ten percent for M equal to 4 or 9.

$$W_M \approx (0.382) \frac{dM(N_D - N_D^{\frac{1}{2}})}{(M^{\frac{1}{2}}-1)} \quad [C-7]$$

## C.3 SAVING IN WIRE LENGTH FOR $M \neq N_D$

One final useful equation is a closed form expression for the saving in wire length as a function of M compared to  $M = N_D$ . This equation is found by dividing [C-5] by [C-7]:

$$\frac{W_{N_D}}{W_M} = \frac{\frac{N_D}{(N_D^{\frac{1}{2}}-1)}}{\frac{M}{(M^{\frac{1}{2}}-1)}} = \frac{N_D}{M} \frac{(M^{\frac{1}{2}}-1)}{(N_D^{\frac{1}{2}}-1)} \approx \left(\frac{N_D}{M}\right)^{\frac{1}{2}} \text{ for large } M \quad [C-8]$$